Vibration Analysis of Flapping Wing Micro Air Vehicle Using Finite Element Methods

A. Dr. M Afzaal Malik, B. Munzer Shahir Ahmed Qureshi

Abstract - *T*his paper illustrates the vibration analysis of flapping wing MAV, using FEM analysis. The wing is modeled using beam and membrane elements. The wing's natural frequencies are computed by modeling the membrane as plate without pre tension and initial bending. Whole wing geometry is modeled and analyzed using eBeam26 and ePlate36[2]. The code for FEM analysis and finding the mode shapes is written in Matlab with the help of guide lines provided in reference-1. Aerodynamic loads used in the FEM analysis are derived from modified strip theory based on blade elemental analysis for semi-elliptical wing[3]. Moreover the wing is also modeled in ANSYS and mode shapes are also found. Finally modes shapes obtained from both software are compared.

I. INTRODUCTION

The growing interest in unmanned aircraft, especially for surveillance in constrained areas, has triggered much research in the area of micro air vehicles (MAVs). Sensors and actuators are becoming smaller and smarter, enabling new aircraft designs. MAVs offer the potential to fly reconnaissance missions in constrained areas, which are difficult for larger aircraft to accomplish. Their small size allows them to navigate in tight corners at low speeds and blend in with their surroundings. The opportunity exists to build low cost systems that can hover or take off in short distances, generate less noise, and be quickly deployed in the field[4] .

In 1997, the Defense Advanced Research Projects Agency (DARPA) initiated a program to develop and test MAVs for military surveillance and reconnaissance missions. DARPA defined the MAV in terms of size, gross weight, and payload – requiring that the maximum dimension in any direction be no greater than 15 cm, the gross weight should not exceed 100 gram, with up to 20 gram devoted to payload, and the MAV should be able to reach altitudes of up to 100m. These MAVs took the form of fixed-wing, rotary-wing, and flapping-wing configurations, among others. Most operated below chord-based Reynolds numbers of 100,000, where conventional aerodynamic theories are inadequate. The Reynolds number is a ratio of inertial to viscous aerodynamic forces used to characterize flight regimes.

Re = Inertial forces/Viscous Forces

DARPA's current MAV initiative is the Advanced Concept Technology Demonstration phase, which seeks to further develop practical MAV systems for military use. Whereas the initial phase focused on individual components in MAV flight, the current phase focuses on technologies that will allow MAVs to accomplish missions in restricted environments with autonomous or semi-autonomous control. These technologies focus on navigation, communications, and multi-task subsystems, particularly because MAV missions could require navigation inside building, in densely populated areas, or in mountainous terrain, caves, or heavily forested areas. Other MAV mission might include sensor dispersal, border surveillance, electronic jamming, communications, counter-drug operations, mine detection, mine detection, and biological and chemical agent detection.

II. MATHEMATICAL DERIVATIONS

Governing equations are to be derived using the extended Hamilton principle, which states that[1&2]

$$0 = \int_0^t (\delta T - \delta \Pi + \delta W_{nc})dt \qquad \text{........(1)}$$

where t is the time, δT is the variation of kinetic energy, $\delta \Pi$ is he variation of elastic energy, and δW_{nc} is the variation of non-conservative work due to aerodynamic loads.

Beam Deformed Reference Line &Initial curvatures

For a naturally curved and twisted beam, three coordinate systems are needed for describing its deformation, as shown in Fig. 1. The system *xyz* is an orthogonal curvilinear coordinate system, where the axis *x* denotes the undeformed reference line of the beam and *s* is the undeformed arc length from the root of the beam to the reference point on the observed cross section. The system *abc* is a rectangular coordinate system attached to the beam root and is used for reference in calculating initial curvatures. Moreover, the system $\xi\eta\zeta$ is a local orthogonal curvilinear coordinate system, where the axis ξ represents the deformed reference line and the axes η and ζ represent the deformed configurations of the axes *y* and *z* if the cross section does not warp. Moreover, $\mathbf{i}_x$, $\mathbf{i}_y$, and $\mathbf{i}_z$ are unit vectors undeformed reference line of the beam and *s* is the undeformed arc length from the root of the beam to the reference point on the observed cross section. The system *abc* is a rectangular coordinate system attached to the beam root and is used for reference in calculating initial curvatures. Moreover, the system $\xi\eta\zeta$ is a local orthogonal curvilinear coordinate system, where the axis ξ represents the deformed reference line and the axes η and ζ represent the deformed configurations of the axes y and z if the cross section does not warp. Moreover, i_x, i_y, and i_z are unit vectors along the axes x, y, and z, respectively; i_a, i_b, and i_c

are unit vectors along the axes a, b, and c, respectively; and i_1, i_2, and i_3 are unit vectors along the axes ξ, η, and ζ, respectively. It can be shown that [2]

$$\begin{Bmatrix} i_x \\ i_y \\ i_z \end{Bmatrix} = [T^0] \begin{Bmatrix} i_a \\ i_b \\ i_c \end{Bmatrix}, \qquad \frac{d}{ds}\begin{Bmatrix} i_x \\ i_y \\ i_z \end{Bmatrix} = [k]\begin{Bmatrix} i_x \\ i_y \\ i_z \end{Bmatrix} \qquad \text{where}$$

$$[k] \equiv \begin{bmatrix} i_x'.i_x & i_x'.i_y & i_x'.i_z \\ i_y'.i_x & i_y'.i_y & i_y'.i_z \\ i_z'.i_x & i_z'.i_y & i_z'.i_z \end{bmatrix} = \begin{bmatrix} 0 & k_3 & -k_2 \\ -k_3 & 0 & k_1 \\ k_2 & -k_1 & 0 \end{bmatrix} = \frac{d[T^0]}{ds}[T^0]^T .. (2)$$

where $[T^0(s)]$ is a known transformation matrix relating the coordinate systems abc and xyz, [k(s)] is the initial curvature matrix, $()' \equiv \partial() / \partial s$, k_1 is the initial twisting curvature, and k_2 and k_3 are the initial bending curvatures. Moreover, the deformed coordinate system ξηζ and the undeformed coordinate system xyz are related by the transformation matrix [T] as

$$\begin{Bmatrix} i_1 \\ i_2 \\ i_3 \end{Bmatrix} = [T]\begin{Bmatrix} i_x \\ i_y \\ i_z \end{Bmatrix}, \quad [T] \equiv \begin{bmatrix} T_{11} & T_{12} & T_{13} \\ T_{21} & T_{22} & T_{23} \\ T_{31} & T_{32} & T_{33} \end{bmatrix}$$

$$= \begin{bmatrix} 1 & 0 & 0 \\ 0 & cos\phi & sin\phi \\ 0 & -sin\phi & cos\phi \end{bmatrix}\begin{bmatrix} T_{11} & T_{12} & T_{13} \\ -T_{12} & T_{11}+\frac{T_{13}^2}{1+T_{11}} & \frac{-T_{12}T_{13}}{1+T_{11}} \\ -T_{13} & \frac{-T_{12}T_{13}}{1+T_{11}} & T_{11}+\frac{T_{12}^2}{1+T_{11}} \end{bmatrix} \quad......(3)$$

Where

$$T_{11} = \frac{1+u'-vk_3+wk_2}{1+e}, T_{12} = \frac{v'+uk_3-wk_1}{1+e}, T_{13} = \frac{(w'-uk_2+vk_1)}{1+e}......(3a)$$

$$e = \sqrt{((1+u'-vk_3+wk_2)^2+(v'+uk_3-wk_1)^2+(w'-uk_2+vk_1)^2)}-1$$

$$T_{21} = -cos\phi T_{12} - sin\phi T_{13}, \quad T_{31} = sin\phi T_{12} - cos\phi T_{13}..........(3b)$$

$$T_{22} = cos\phi\left(T_{11}+\frac{T_{13}^2}{1+T_{11}}\right) - sin\phi\frac{T_{12}T_{13}}{1+T_{11}},$$

$$T_{32} = -sin\phi\left(T_{11}+\frac{T_{13}^2}{1+T_{11}}\right) - cos\phi\frac{T_{12}T_{13}}{1+T_{11}}$$

$$T_{23} = sin\phi\left(T_{11}+\frac{T_{12}^2}{1+T_{11}}\right) - cos\phi\frac{T_{12}T_{13}}{1+T_{11}}$$

$$T_{33} = cos\phi\left(T_{11}+\frac{T_{12}^2}{1+T_{11}}\right) + sin\phi\frac{T_{12}T_{13}}{1+T_{11}}$$

Deformed Curvatures

Here, u, v, and w are the displacements of the reference point on the observed cross section with respect to the axes x, y, and z, as shown in Fig. 1. Moreover, φ is an Euler angle related to the twisting angle of the observed cross section with respect to the deformed reference axis ξ , and e is the axial strain along the axis ξ . It follows from (3) that T_{2i} and T_{3i} can be represented in terms of , T_{11} T_{12} , T_{13} , and φ , as shown in Eq. (3b). Differentiating Eq. (3) with respect to s and using Eq. (2) and $[T]^{-1} = [T]^T$ yields

$$\frac{\partial}{\partial s}\begin{Bmatrix} i_1 \\ i_2 \\ i_3 \end{Bmatrix} = [K]\begin{Bmatrix} i_1 \\ i_2 \\ i_3 \end{Bmatrix}, [K] \equiv \begin{bmatrix} 0 & \rho_3 & -\rho_2 \\ -\rho_3 & 0 & \rho_1 \\ \rho_2 & -\rho_1 & 0 \end{bmatrix} = [T]'[T]^T + [T][k][T]^T$$

where ρ_1 is the deformed twisting curvature and ρ_2 and ρ_3 are the deformed bending curvatures. Note that ρ_i are not real curvatures because the differentiation is with respect to the undeformed differential length ds, instead of the deformed length (1+ e)ds . Using Eqs. (4), (3), and (2), one can show that

$$\rho_1 = i_2'.i_3 = \phi' + \frac{1}{(1+e)(1+T_{11})}\left[T_{13}(v'+uk_3-wk_1)'-T_{12}(w'- uk_2+vk_1)'\right] + T_{11}k_1 + T_{12}k_2 + T_{13}k_3$$

$$\rho_2 = -i_1'.i_3 = -\frac{1}{1+e}\left[T_{31}(u'-vk_3+wk_2)' + T_{32}(v'+uk_3 wk_1)' + T_{33}(w'-uk_2+vk_1)'\right] + T_{21}k_1 + T_{22}k_2 + T_{23}k_3$$

$$\rho_3 = i_1'.i_2 = \frac{1}{1+e}\left[T_{21}(u'-vk_3+wk_2)'+T_{22}(v'+uk_3-wk_1)' + T_{23}(w'-uk_2+vk_1)'\right] + T_{31}k_1 + T_{32}k_2 + T_{33}k_3$$

$$............ (5)$$

For a geometrically exact beam theory, fully nonlinear stress-strain and strain-displacement relations are given by[2]

$$\{J\} = [\bar{Q}]\{B\}, \{J\} \equiv \begin{Bmatrix} J_{11} \\ J_{12} \\ J_{13} \end{Bmatrix}, \{B\} \equiv \begin{Bmatrix} B_{11} \\ 2B_{12} \\ 2_{B_{13}} \end{Bmatrix} \& \ [\bar{Q}] = \begin{bmatrix} E & 0 & 0 \\ 0 & G & 0 \\ 0 & 0 & G \end{bmatrix}$$

$$\{B\} = [S]\{\Psi\}, \{\delta B\} = [S]\{\delta \Psi\},$$

$$\{\Psi\} \equiv \{e, \gamma_6, \gamma_5, \rho_1-k_1, \rho_2-k_2, \rho_3-k_3, \gamma_6', \gamma_5'\}^T$$

$$[S] \equiv \begin{bmatrix} 1 & 0 & 0 & 0 & z & -y & y & z \\ 0 & 1+yk_3 & zk_3 & -z & 0 & 0 & 0 & 0 \\ 0 & -yk_2 & 1-zk_2 & y & 0 & 0 & 0 & 0 \end{bmatrix}$$

$$\begin{Bmatrix} \delta e \\ (1+e)\delta\theta_3 \\ -(1+e)\delta\theta_2 \end{Bmatrix} = [T]\begin{Bmatrix} \delta u' \\ \delta v' \\ \delta w' \end{Bmatrix} - [T][k]\begin{Bmatrix} \delta u \\ \delta v \\ \delta w \end{Bmatrix},$$

$$\begin{Bmatrix} \delta\rho_1 \\ \delta\rho_2 \\ \delta\rho_3 \end{Bmatrix} = \begin{Bmatrix} (\delta\theta_1)' \\ (\delta\theta_2)' \\ (\delta\theta_3)' \end{Bmatrix} - [K]\begin{Bmatrix} \delta\theta_1 \\ \delta\theta_2 \\ \delta\theta_3 \end{Bmatrix}$$

$$\delta\theta_1 = \delta\phi + \frac{T_{13}k_3+T_{12}k_2}{1+e+T_{11}+eT_{11}}\delta u - \frac{T_{12}k_1}{1+e+T_{11}+eT_{11}}\delta v - \frac{T_{13}k_1}{1+e+T_{11}+eT_{11}}\delta w + \frac{T_{13}}{1+e+T_{11}+eT_{11}}\delta v' - \frac{T_{12}}{1+e+T_{11}+eT_{11}}\delta w'$$

where J_{ij} are Jaumann stresses, B_{ij} are Jaumann strains, E is Young's modulus, G is the shear modulus, and γ_5 and γ_6 are transverse shear strains.

Membrane

For an initially curved membrane, three coordinate systems are also needed for describing its deformation, as shown in Fig. 4. The system xyz is an orthogonal curvilinear coordinate system with the curvilinear axes x and y being on the undeformed reference surface and the z axis being a rectilinear axis. The system abc is a rectangular coordinate system used for reference purpose in the calculation of initial curvatures. The system ξηζ is a local orthogonal curvilinear coordinate system with the curvilinear axes ξ and η being on the deformed reference surface and the Type equation here.ζ axis being a rectilinear axis. Moreover, j_1, j_2 , and j_3 are unit vectors along the axes x, y, and z, respectively; i_a, i_b, and i_c are unit vectors along the axes a, b, and c, respectively; and i_1, i_2, and i_3 are unit vectors along the axes ξ, η, and ζ, respectively. For a geometrically exact membrane theory, fully nonlinear stress-strain and strain-displacement relations are given by [1,2]

$$\{J\} = [\bar{Q}]\{B\}, \{J\} \equiv \begin{Bmatrix} J_{11} \\ J_{12} \\ J_{13} \end{Bmatrix}, \{B\} \equiv \begin{Bmatrix} B_{11} \\ B_{22} \\ 2_{B_{12}} \end{Bmatrix}, [\bar{Q}] = \frac{E}{1-v^2}\begin{bmatrix} 1 & v & 0 \\ v & 1 & 0 \\ 0 & 0 & \frac{1-v}{2} \end{bmatrix} \quad (7)$$

$$\{B\} = \{\Psi\} \equiv \{(1+e_1)cos\gamma_{61} - 1, (1+e_2)cos\gamma_{62} - 1, (1+e_1)sin\gamma_{61} + (1+e_2)sin\gamma_{62}\}^T$$

$$e_1 = \sqrt{(1+u_x-vk_5^0+wk_1^0)^2+(v_x+uk_5^0+wk_{61}^0)^2+(w_x-uk_1^0-vk_{61}^0)^2} - 1$$

$$e_2 = \sqrt{(u_y-vk_4^0+wk_{62}^0)^2+(1+v_y+uk_4^0+wk_2^0)^2+(w_y-uk_{62}^0-vk_2^0)^2} - 1$$

$$\gamma_6 = \gamma_{61} + \gamma_{62} = \sin^{-1}(\hat{T}_{11}\hat{T}_{21} + \hat{T}_{12}\hat{T}_{22} + \hat{T}_{13}\hat{T}_{23}) \qquad (7a)$$

$$\gamma_{61} = \tan^{-1}\left(\frac{(1+e_2)sin\gamma_6}{1+e_1+(1+e_2)cos\gamma_6}\right), \gamma_{62} = \tan^{-1}\left(\frac{(1+e_1)sin\gamma_6}{1+e_2+(1+e_1)cos\gamma_6}\right)$$

$$\hat{T}_{11} = \frac{1+u_x-vk_5^0+wk_1^0}{1+e_1}, \hat{T}_{12} = \frac{v_x+uk_5^0+wk_{61}^0}{1+e_1}, \hat{T}_{13} = \frac{w_x-uk_1^0-vk_{61}^0}{1+e_1} \qquad (7b)$$

$$\hat{T}_{21} = \frac{u_y-vk_4^0+wk_{62}^0}{1+e_2}, \hat{T}_{22} = \frac{1+v_y+uk_4^0+wk_2^0}{1+e_2}, \hat{T}_{23} = \frac{w_y-uk_{62}^0-vk_2^0}{1+e_2}$$

Here ν is Poisson's ratio, k_i^0 are initial curvatures, u, v,w are displacement components of an arbitrary point on the reference plane, and $u_x \equiv \partial u / \partial x$, $u_y \equiv \partial u / \partial y$, etc. It can be shown that the variations of extension strains e_1 and e_2 and shear strain $\gamma_6 (= \gamma_{61} + \gamma_{62})$ on the reference plane of the membrane are given

$$\delta e_1 = \hat{T}_{11}\delta t_{11} + \hat{T}_{12}\delta t_{12} + \hat{T}_{13}\delta t_{13}, \quad \delta e_2 = \hat{T}_{21}\delta t_{21} + \hat{T}_{22}\delta t_{22} + \hat{T}_{23}\delta t_{23}$$

$$\delta\gamma_6$$
$$= \frac{(\hat{T}_{21} - sin\gamma_6\hat{T}_{11})\delta t_{11} + (\hat{T}_{22} - sin\gamma_6\hat{T}_{12})\delta t_{12} + (\hat{T}_{23} - sin\gamma_6\hat{T}_{13})\delta t_{13}}{cos\gamma_6(1+e_1)}$$
$$+ \frac{(\hat{T}_{11} - sin\gamma_6\hat{T}_{21})\delta t_{21} + (\hat{T}_{12} - sin\gamma_6\hat{T}_{22})\delta t_{22} + (\hat{T}_{13} - sin\gamma_6\hat{T}_{23})\delta t_{23}}{cos\gamma_6(1+e_2)}$$

$$\delta\gamma_{61} = \frac{(1+e_2)cos\gamma_{62}\delta\gamma_6 - sin\gamma_{61}\delta e_1 + sin\gamma_{62}\delta e_2}{cos\gamma_{61}(1+e_1)+cos\gamma_{62}(1+e_2)}, \qquad (8)$$

$$\delta\gamma_{62} = \frac{(1+e_1)cos\gamma_{61}\delta\gamma_6 + sin\gamma_{61}\delta e_1 - sin\gamma_{62}\delta e_2}{cos\gamma_{61}(1+e_1)+cos\gamma_{62}(1+e_2)}$$

$$\delta t_{11} = \delta u_x - k_5^0\delta v + k_1^0\delta w, \qquad \delta t_{12} = \delta v_x + k_5^0\delta u + k_{61}^0\delta w,$$
$$\delta t_{13} = \delta w_x - k_1^0\delta u - k_{61}^0\delta v$$
$$\delta t_{21} = \delta u_y - k_4^0\delta v + k_{62}^0\delta w, \qquad \delta t_{22} = \delta v_y + k_4^0\delta u + k_2^0\delta w$$
$$\delta t_{23} = \delta w_y - k_{62}^0\delta u - k_2^0\delta v$$

For both beam and membrane elements, it follows from Eqs. (6), (7a,b), and (8) that

$$\{\delta\Psi\} = [\Psi]\{\delta U\}, \Psi_{ij} = \frac{\delta\Psi_i}{\delta U_j} \qquad (9)$$

Where

Beam $\{U\} \equiv \{U_1\} = \{u, u', u'', v, v', v'', w, w', w'', \phi, \phi', \gamma_5, \gamma_5', \gamma_6, \gamma_6'\}^T$ (9a)

Membrane: $\{U\} \equiv \{U_1\} = \{u, u_x, u_y, v, v_x, v_y, w, w_x, w_y\}^T$ (9b)

The way the components of $\{U\}$ are approximated defines a specific finite element. Using the finite-element discretization scheme, one can discretize the displacements as

Beam: $\{u, v, w, \phi, \gamma_5, \gamma_6\}^T = [N_1]\{q_1^{[j]}\}$ where $\{q_1^{[j]}\}$ ....(10)

$= \{u_i, v_i, w_i, \phi_i, w_i', v_i', u_i', \gamma_{5i}', \gamma_{6i}, u_k, v_k, w_k, \phi_k, w_k', v_k', u_k', \gamma_{5k}', \gamma_{6k}\}^T$

Membrane: $\{u, v, w\}^T = [N_2]\{q_2^{[j]}\}$ and

$\{q_2^{[j]}\} = \{u_i, v_i, w_i, u_k, v_k, w_k, u_l, v_l, w_l\}^T$

where $\{q_1^{[j]}\}$ is the displacement vector of the jth beam element and $[N_1]$ is a 6×18 matrix of 1D shape functions, and $\{q_2^{[j]}\}$ is the displacement vector of the jth membrane element and $[N_2]$ is a 3×9 matrix of 2D shape functions. Substituting Eq. (10) into Eqs. (9a,b) yields

Beam: $\{U_1\} = [D_1]\{q_1^{[j]}\}$ and $[D_1] \equiv [\delta_1][N_1]$ (10a)

Membrane: $\{U_2\} = [D_2]\{q_2^{[j]}\}$ and $[D_2] \equiv [\delta_2][N_2]$ (10b)

where $[\partial_1]$ is a 15×6 matrix and $[\partial_2]$ is a 9×3 matrix consisting of differential operators. For beams, the variation of elastic energy is given by

Beam:
$$\delta\Pi =$$
$$\int_V \{\delta B\}^T\{J\}dV =$$
$$\sum_{j=1}^N \int_{L[j]}\{q_1^{[j]}\}^T[D_1]^T[\Psi]^T[\phi_1]\{\Psi\}ds = \sum_{j=1}^N \{q_1^{[j]}\}^T[K_1^{[j]}]\{q_1^{[j]}\}, \qquad (11)$$
$$[K_1^{[j]}]\{q_1^{[j]}\} \equiv \int_{L[j]}[D_1]^T[\Psi]^T[\phi_1]\{\Psi\}ds, \quad [\phi_1] \equiv \int_A[S]^T[\bar{Q}][S]dA$$

Where V is the volume, N_e is the total number of elements, $[L^{[j]}]_j$ is the length of the jth element, and $[K^{[j]}]$ is the stiffness matrix of the *j*th beam element. For membranes, the variation of elastic energy is given by

Membrane:
$$\delta\Pi = \sum_{j=1}^N \int_{A^{[j]}}\{q_2^{[j]}\}^T[D_2]^T[\Psi]^T[\phi_2]\{\Psi\}dA = \sum_{j=1}^N \{q_2^{[j]}\}^T[K^{[j]}]\{q_2^{[j]}\}$$
$$[K_2^{[j]}]\{q_2^{[j]}\} \equiv \int_{A^{[j]}}[D]^T[\Psi]^T[\phi_2]\{\Psi\}dA, \quad [\phi_2] = \int_{-\frac{h}{2}}^{\frac{h}{2}}[\bar{Q}]dz \qquad (12)$$

where N_e is the total number of elements, $A^{[j]}$ is the area of the jth element, and $[K_2^{[j]}]$ is the stiffness matrix of the *j*th membrane element.

The variation of kinetic energy is given by
$$\delta T = -\int_V \rho(\ddot{u}\delta u + \ddot{v}\delta v + \ddot{w}\delta w)dV \qquad (13)$$
where ρ is the mass density. Only translational inertias are included because rotary inertias are assumed to be negligible for the thin rods and membranes used in an MAV. It follows from Eq. (18) that the variation of non-conservative energy due to aerodynamic loads is given by
$$\delta W_{nc} = \int_A (r_1\delta u + r_2\delta v + r_3\delta w)dA = \int_A \{\delta u \ \delta v \ \delta w\}\{r_1 \ r_2 \ r_3\}^T dA =$$
$$\sum_{j=1}^N \{\delta q^{[j]}\}^T\{R^{[j]}\} = \{\delta q\}^T\{R\} \qquad (14)$$
where r_1, r_2, and r_3 are distributed external loads per unit area along the axes x, y and z , respectively. $\{R^{[j]}\}$ is the elemental nodal loading vector, and $\{R\}$ is the structural nodal loading vector. Furthermore,
$$\{R^{[j]}\} \equiv \int_{A^{[j]}}[N_2]^T\{r_1 \ r_2 \ r_3\}^T dA \qquad (15)$$

III. RESULTS AND FIGURES

Before doing the analysis in the Matlab and ANSYS we have to carry out the initial sizing of the ornithopter. Based on the span of the ornithopter, initial parameters can be calculated from following empirical formulae [5]:-

$$Mass = M = 0.606 \ (2B)^{2.381} \ to \ 0.885 \ (2B)^{2.381}$$
$$Flapping \ Frequency = f = 3.03 \ (M)^{-0.36}$$
$$Aspect \ Ratio = AR = 7.83 \ (M)^{0.05} \ to \ 8.15 \ (M)^{0.05}$$

For an ornithopter with span of 40 cm, the calculated initial value of flapping frequency is 6.96 Hz to 7.97 Hz and AR is 6.84 to 7.25. The selected root chord is 8 cm, which gives AR just above 6.2, because the above equations are just initial guess.

A MATLAB code has been written for Elliptical wing model[2].In this code eBeam26 and ePlate 36[2] are used and linear analysis is done. Modal analysis is done and Mode shapes are obtained. This code has 8 inputs namely a) Linear Analysis b) Modal Analysis c) Element d) Number of natural Frequencies

to be computed e) Mode shape plotting f) Mode number g) Magnification factor h) Frequency response function. There are also some options for plotting results like i) Original undeformed geometry ii) Mode shapes.

The same wing is analyzed in ANSYS using Beam188 and Shell181 elements. Modal/analysis is done and these modes are compared with those obtained in Matlab.
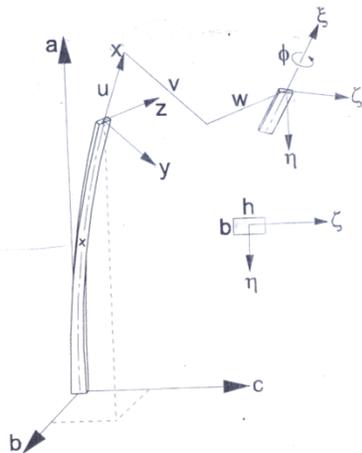

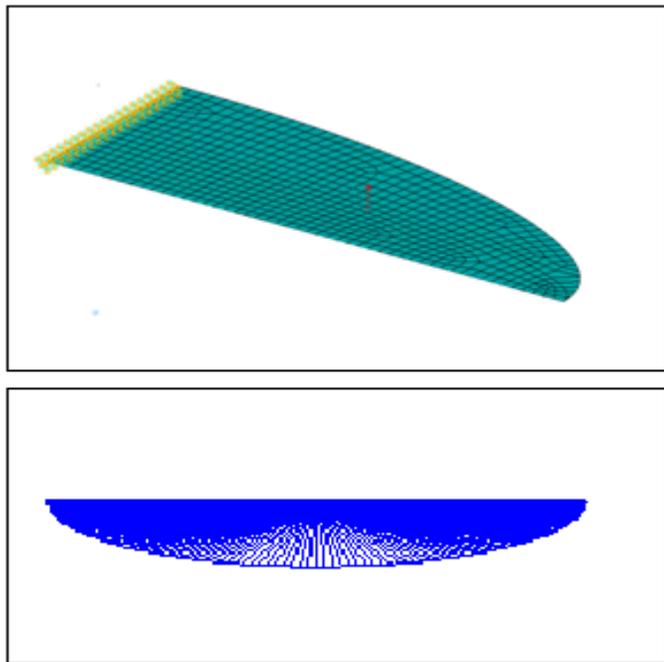Fig 1: Coordinate system and displacement variables for initially curved beam

Fig 2: In this figure wing geometries modeled in Ansys and Matlab are shown. Upper geometry shown is undeformed geometry modeled in ANSYS and the lower one is the same modeled in Matlab

.
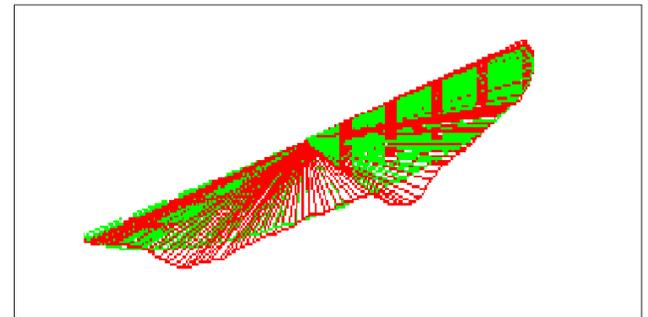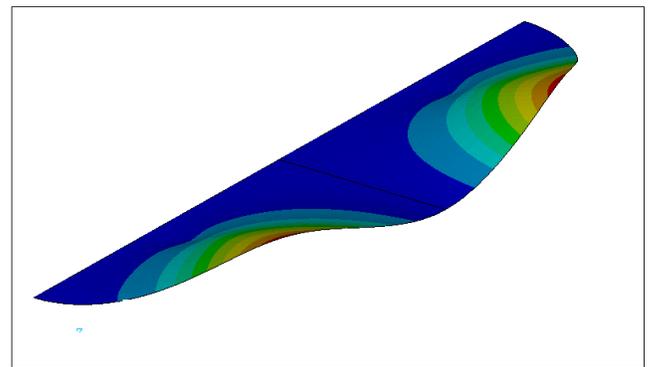
Fig 3: First vibration modes obtained from ANSYS and Matlab are presented in this figure. Upper mode shape of this figure is the first vibration mode obtained in ANSYS at 0Hz and lower one is the same mode obtained in Matlab at 0 Hz.
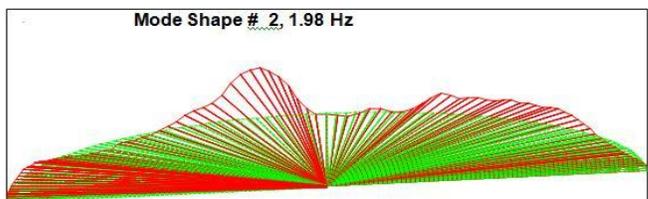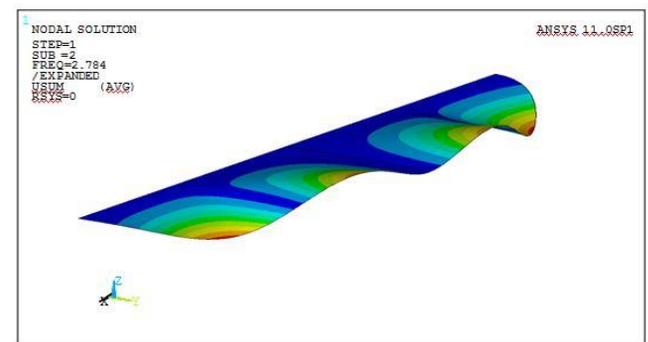

Fig 4: In this figure second vibration mode shape is shown which is obtained through both software ANSYS and Matlab. Upper mode shape of this figure is the second vibration mode obtained in ANSYS at 2.74Hz and lower one is the same mode obtained in Matlab at 1.98 Hz. There is little frequency difference between the modes obtained from the two software. This difference can be minimized by refining the codes further as a future work
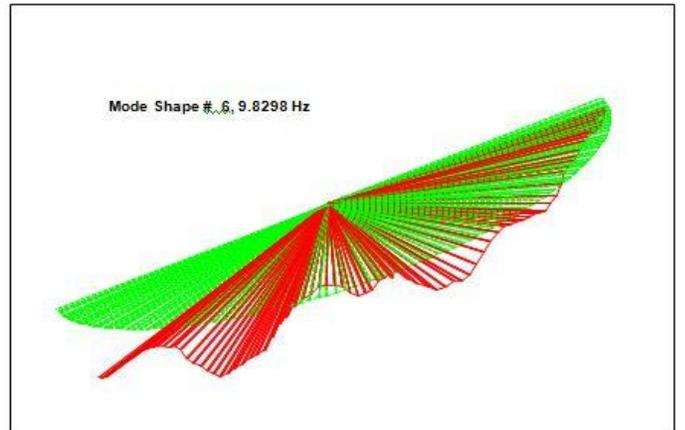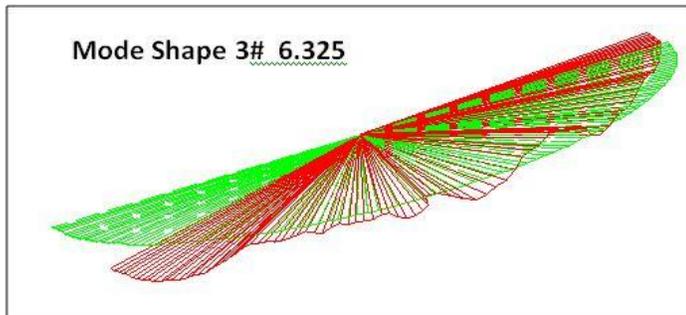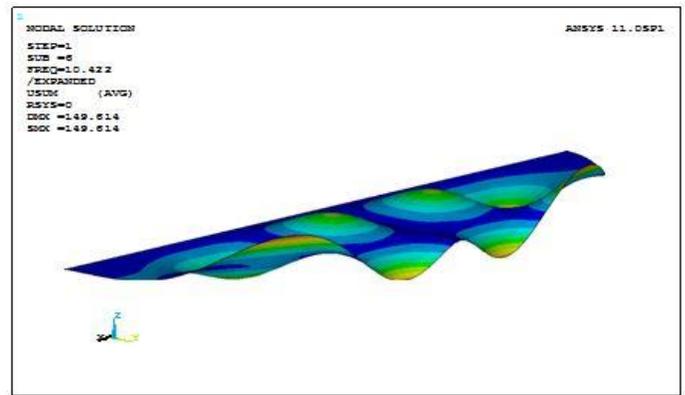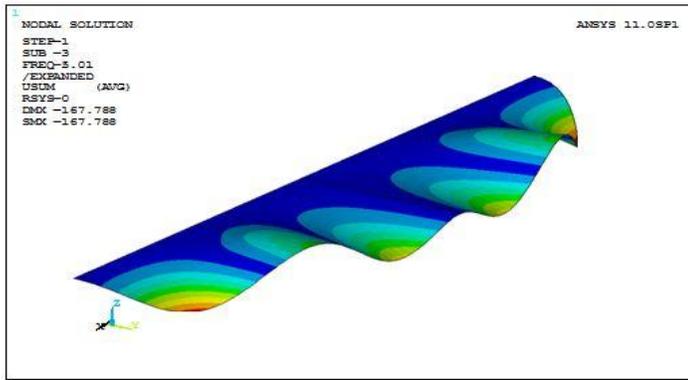
.

Fig 5: In this figure third vibration mode of wing has been shown found through both ANSYS and Matlab software. Upper mode shape shown in this figure is third vibration mode found in ANSYS at the frequency 5.01 Hz whereas lower one is the same mode shape found in Matlab at 6.325 Hz frequency. Both bending and torsional modes are visible in these mode shapes.

Fig 6: In this figure sixth vibration mode of wing has been shown which has been obtained in both software ANSYS and Matlab. Mode shape shown in the upper of this figure is that obtained in ANSYS at 10.42 Hz frequency where as lower one is the same mode shape found in Matlab at 9.82 Hz frequency. Both bending and torsional modes are visible in these mode shapes.

REFERENCES

[1] P.Frank Pai, Dar YaK. Chernova, 2009 *"Nonlinear Modeling and Vibration Characterization of MAV Flapping Wings",*

[2] P.Frank Pai, 2006. Highly Flexible Sructures: Modeling, Computation and Experimentation, 1st ed., American Institute of Aeronautics and Austronautics, Inc. 1801 Alexander Bell Drive, Reston, VA 20191.

[3] M. Afzaal Malik, Farooq Ahmed, *"Effect of Different Design Parameters on Lift, Thrust and Drag of an Ornithopter ",* ICME 2010.

[4] Beverly Beassley, Masters of Science,2006, *"A study Of Planar and Nonplanar Membrane Wing Planforms for the Design of a Flapping Wing Micro Air Vehicle",* Master Thesis University of Maryland.

[5] Norberg, U.M., *"Vertebrate Flight"*, Springer-Verlag, Berlin, 1990, pp. 166-179

[6] R.J.Wooten, 2003*"Approaches to the structural modeling of ect wings"The Royal Society Trans. R .Soc London

[7] DeLaurier, J.D., *"An Aerodynamic Model for Flapping Wing Flight,"* The Aeronautical Journal of the Royal Aeronautical Society, April 1993, pp. 125-130.

[8] Hirotaka Natsume, *"Experimental Study of High Propulsive Efficiency of Three Dimensional Flapping Wing"*, Kyushu University, Fukuoka, Japan.

[9] Mueller, T.J., *"Fixed and Flapping Wing Aerodynamics for Micro Air Vehicle Applications"*, Reston, VA: AIAA, 2001.